Proceedings of the Seventh International Conference on
Railway Technology: Research, Development and Maintenance
Edited by: J. Pombo
Civil-Comp Conferences, Volume 15, Paper 23.5
Civil-Comp Press, Edinburgh, United Kingdom, 2026
ISSN: 2753-3239, doi: 10.4203/ccc.15.23.5

Comparison of Refueling Methods for Hydrogen Rail Vehicles

L. Brünner, S. Wieser, A. Roß and M. Böhm

Institute of Vehicle Concepts, German Aerospace Center, Berlin/Stuttgart, Germany

Abstract

Hydrogen-powered rail vehicles offer a viable solution for decarbonizing non-electrified regional rail networks. This study evaluates different hydrogen refueling strategies, focussing on refueling performance and safety compliance. A lumped-parameter simulation model, validated against real-world data from the "Wasserstoffschiene Heidekrautbahn" project, is used to compare trailer-based refueling, ramp rate refueling and MC Formula-based (MCF) refueling with and without vehicle-to-station communication. These methods allowed for an end of fill SoC ranging from 56 % to 100 %, with a maximum refueling speed of 5.3 %/min and completion in under 14 min. Furthermore, the results show that trailer refueling offers flexibility and fast initial fills, but its performance degrades over consecutive cycles due to reduced trailer pressure, limiting the achievable vehicle SoC. Segmented trailers improve consecutive refueling capability but at the cost of slightly slower initial fills. Compared to table-based refueling, the MCF method without communication achieves a lower SoC due to early termination caused by a steeper ramp rate. In contrast, MCF with communication enables complete refueling to 100 % SoC. The findings highlight that vehicle-to-station communication is essential for efficient and reliable hydrogen refueling in rail transport and underscore the need for updated standards to support its implementation.

Keywords: Heidekrautbahn, hydrogen, multiple units, refueling, simulation, modeling.

1 Introduction

At present, only around 54 % of all railway lines in Germany are electrified, yet these lines carry around 90 % of all rail transport services. At around 80 %, local rail passenger transport has the lowest proportion of electrified transport services compared to freight and long-distance passenger transport. [1] Electrification of the currently non-electrified branch lines, on which around 20 % of regional rail transport services are provided, is therefore not usually worthwhile from an economic point of view, meaning that these are still served by diesel-powered rail vehicles. Alternatively powered rail vehicles – such as battery and hydrogen trains – offer a possible/viable solution here.

Hydrogen trains have been in regular operation in various regions across Germany since 2022. [2] As part of the publicly funded project “Wasserstoffschiene Heidekrautbahn”, seven hydrogen multiple units (HEMU) of type Siemens Mireo Plus H (see Figure 1 left) have been put into operation in the Berlin-Brandenburg metropolitan region since end of 2024. The trains are operated on the so called “Heidekrautbahn”, which is located north of Berlin (see Figure 1 right). [3]

Figure 1: left – Siemens Mireo Plus H [4]; right – route of the Heidekrautbahn [5]

The main goal of the “Wasserstoffschiene Heidekrautbahn” project is to enable an emission free regional rail transport using green hydrogen produced from local wind and solar energy. This is achieved by building up the necessary infrastructure to refuel the trains as well as a local hydrogen production. Involved in the project are the energy company ENERTRAG, which is responsible for the hydrogen production, the Niederbarminer Eisenbahn, who are the responsible vehicle operator as well as the Kreiswerke Barnim, who built and operate the hydrogen refueling station. Furthermore, the project is supported with accompanying research by the

Brandenburg University of Technology and the Institute of Vehicle Concepts of the German Aerospace Centre. [3], [6]

Hydrogen trains like the Mireo Plus H store hydrogen in pressurized tanks with a pressure level of 35 MPa (H35), giving them a similar range to diesel trains. However, the hydrogen heats up during refueling due to the compression in the tanks and the negative Joule-Thomson coefficient of the hydrogen. In order to prevent the hydrogen tanks from being damaged due to excessive thermal stress and to ensure the operational safety of the tanks over the vehicle service life of 30 years, a maximum temperature of 85 °C is required in the tanks during refueling. Various refueling protocols have been developed to comply with this limit (see Table 1).

Table 1: Overview of existing refueling protocols for the 35 MPa pressure level [7], [8], [9], [10]

Standard	**max. H2-mass**	**Pre-Cooling**	**max. Mass Flow**
SAE J2601	1,2 kg ≤ x ≤ 6 kg	T40 – T20	≤ 60 g/s
SAE J2601-2	purely informative standard, no refueling protocols		
SAE J2601-5 (TIR)	6 kg ≤ x ≤ 180 kg	T40 – TA	≤ 120 g/s
H35 CEP protocol	20 kg ≤ x ≤ 42,5 kg	T40 – TA	≤ 120 g/s

As can be seen in Table 1, there is currently no published standard which can be used to refuel hydrogen (passenger) trains, as those typically have an overall hydrogen capacity of around 200 kg stored in two separate refillable storage systems. The only standard that could be applicable for such amounts is the SAE J2601-5. However, this standard is not yet published as a standard and remains in a pre-standard status (TIR) due to lack of field testing. Therefore, refueling protocols have to be developed specifically for each fleet of hydrogen trains. Furthermore, there is currently no communication used between station and vehicle when refueling these trains. This is due to safety concerns, as the intended interface for communication, which is infrared according to SAE J2799 [11], does not comply with the necessary safety integrity level mandatory for rail vehicles. Consequently, the refueling process has to be done slower than necessary wasting potential for faster refueling.

To ensure that the vehicles do not cause any disadvantages in operation, refueling with hydrogen must achieve refueling speeds close or similar to diesel. In order to show which potential could be gained concerning refueling duration, different refueling approaches are compared in this study. The approaches include a trailer refueling as well as refuelings derived from SAE J2601-5 (table-based, MC-Formula-based with and without communication). For this purpose, simulation models of the refueling process were set up using Dymola and validated using measurement data from the “Wasserstoffschiene Heidekrautbahn” project.

2 Methods

This chapter outlines the key methods used in the research presented. Section 2.1 provides an overview of the vehicle used on the Heidekrautbahn, highlighting essential system characteristics relevant to the modeling approach. Section 2.2 explores the hydrogen refueling model employed in the study. To ensure model reliability and accuracy, section 2.3 presents the model validation process. Finally, section 2.4 discusses the various refueling strategies considered, which will be applied and further analyzed in Chapter 3.

2.1 Heidekrautbahn-Trains

The Siemens Mireo Plus H, operated on the Heidekrautbahn, is a two-car HEMU as shown in Figure 1 (left). Its hydrogen storage system consists of four tank racks, one of which is illustrated in Figure 2. Each rack contains four Type IV hydrogen tanks – two large and two small ones – capable of storing approximately 45 kg of gaseous hydrogen. During refueling, two tank racks are refueled simultaneously. This configuration is reflected in the simulation model shown in Figure 3. [12], [13]

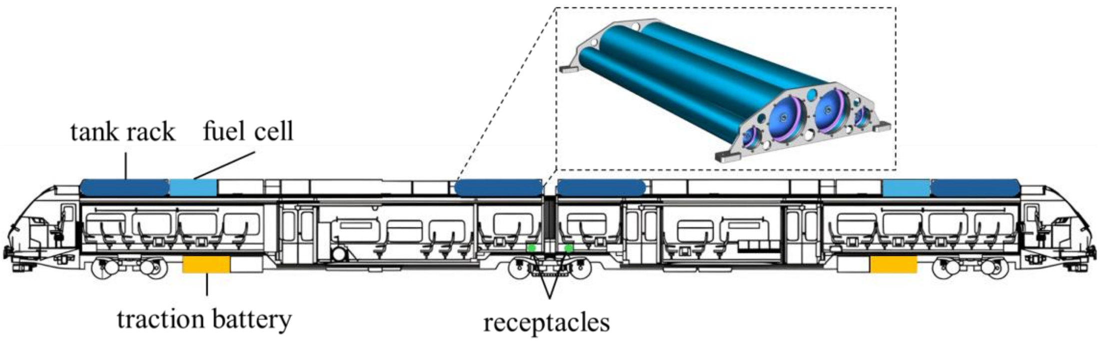

Figure 2: Side view of the Siemens Mireo Plus H including drive train configuration and tank rack (own representation based on [6], [12], [14], [15])

2.2 Hydrogen refueling model

Various approaches to model the hydrogen refueling process can be used. For this research, a lumped-parameter simulation model, which has been previously developed and described in [16] and [17], has been utilized and adapted to suit the Heidekrautbahn-Trains. The model is implemented in Dymola, with its user interface is shown in Figure 3.

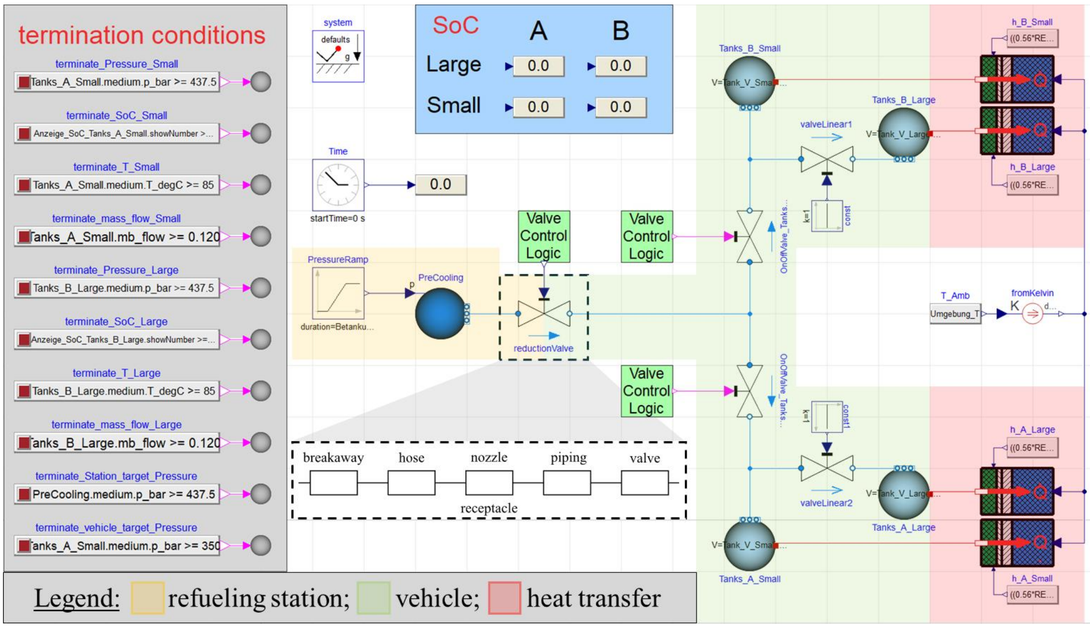

Figure 3: Interface of the main simulation model in Dymola

In the developed simulation model, all relevant components that are located between refueling station and the vehicle are represented by one flow resistance, which is a commonly used approach for hydrogen refueling models (e.g. see [18]). This flow resistance is modeled by using a reduction valve and characterized by a K_V-value (see Table 2). The components represented by this K_V-value are: breakaway, hoses, nozzle, receptacle, piping and valves (see Figure 3).

The simulation model determines the thermodynamic state of hydrogen in the vehicle tanks based on the pressure and temperature at the refueling dispenser. Hydrogen is modeled using the Leachman equations, implemented via the "External Media Library", which relies on the open-source database CoolProp [19]. As hydrogen flows through the system, pressure losses due to flow resistance in the components are accounted for, influencing the state of hydrogen before it enters the vehicle tanks. The hydrogen state within the vehicle tanks is then calculated considering the tanks volume, geometry and heat transfer with the environment. The heat transfer is primarily governed by the tank's design and material properties (see Table 2). It is modeled through custom sub-models that use components from the "Modelica Standard library" as well as the "Modelica Buildings library" [20]. These sub-models consider convective heat transfer between the hydrogen and the inner tank wall, transient heat conduction through the tank wall and convective heat transfer at the outer tank surface. To efficiently represent the vehicle's storage system, identical individual tanks in one tank rack are aggregated into a single equivalent tank with a combined volume and surface area, which significantly reduces computational complexity. The geometry of each individual tank is assumed to be capsule-like, consisting of a cylindrical section with two hemispherical ends.

Other key components of the simulation model are the State of Charge (SoC) calculation, which is based on the following equation [21]:

$$SoC\ (\%) = \frac{\rho(p, T)}{\rho(35\ MPa,\ 15\ °C)} * 100 \qquad 1$$

Furthermore, the valve control logic and termination conditions are integral parts of the simulation model, as seen in Figure 3. The valve control logic manages the automatic opening and closing of the main valve and prevents hydrogen flow between tank racks when their initial pressures differ, thereby avoiding unintended pressure equalization. Termination conditions are implemented to halt the simulation if any safety-critical limits defined in SAE J2601-2 are exceeded. These include a maximum hydrogen temperature of 85 °C, a maximum pressure inside the tanks of 43.75 MPa and a mass flow exceeding 120 g/s. Additionally, the simulation stops if the SoC inside of the tanks exceeds 100 %. Two further conditions are included to enable early termination: one based on a target pressure in the vehicle tanks and another based on target pressure at the refueling station.

For model validation, the vehicle specifications of the Siemens Mireo Plus H are employed. However, for the subsequent comparison of different refueling strategies, a set of publicly available parameters is used. This parameter set is listed in Table 2.

Table 2: Parameterization of the refueling model

Parameter	Value	Source	Parameter	Value	Source
Tank System (= 2 Tank Racks)			**Small and Large Tank**		
K_V	0.2 m^3/h	[17]	Type	IV	[13]
m_{TS}	90 kg	[13]	$m_{H_2,L}$: $m_{H_2,S}$	2:1	sel.
N_S , N_L	4, 4	[13]	$m_{H_2,S}$, $m_{H_2,L}$	7.5 kg, 15 kg	calc.
V_{TS}	3750 L	calc.	V_S , V_L	312.5 L, 625 L	calc.
Trailer			L_S , L_L	3 m, 3 m	sel.
V_T	31.5 m3	[22]	t_{Liner} , t_{CFRP}	5 mm, 15 mm	[18]
N_T	90	[22]	**Trailer Tanks**		
ID	13.1 mm	[23]	Type	IV	[22]
Material Data Type IV Tank / Heat Transfer			V_{TT}	350 L	[22]
ρ_{Liner} , ρ_{CFRP}	945 kg/m^3, 1494 kg/m^3	[18]	r_{TT}	0.25 m	[24]
c_{Liner} , c_{CFRP}	2100 J/(kg K), 1120 J/(kg K)	[18]	L_{TT}	2.36 m	[24]
λ_{Liner} , λ_{CFRP}	0.5 W/(m K), 0.74 W/(m K)	[18]	t_{Liner} , t_{CFRP}	5 mm, 15 mm	[18]
$h_{inner\ Tank\ Wall}$	dynamic	[25]	$P_{nom}(15\ °C)$	350 bar, 500 bar	sel., [22]
$h_{outer\ Tank\ Wall}$	10 W/(m^2 K)	[26]			

*TS – Tank System, S – small, L – Large, T – Trailer, TT – Trailer Tank, ID – Inner Diameter

2.3 Model validation

The developed hydrogen refueling simulation models require validation through comparison with measurement data to ensure their accuracy and reliability. For this purpose, comprehensive datasets were collected during hydrogen refueling operations, both at the refueling station and within the vehicles. At the refueling station, key operational parameters – including ambient temperature, pre-cooling temperature, pressure ramp rate, and hydrogen mass flow rate – were recorded. Within the vehicles, the pressure in each tank rack and the temperature in each individual tank were measured. To ensure consistency between measurements conditions and simulation inputs, the simulation models were adapted accordingly. Ambient temperature, pre-cooling temperature, and the pressure ramp rate were imported as time series directly derived from the measurement data to perform the simulations within the validation process.

Figure 4 illustrates the relative deviations between the measured and simulated values, as well as the temporal evolution of variables: hydrogen mass flow, tank pressure, and tank temperature. As the larger vehicle tanks heat up more, only those are evaluated in this chapter, however, the small tanks behave identically in terms of validation. The relative deviation of the hydrogen mass flow is notably higher compared to those of pressure and temperature. Particularly at the start and end phases of refueling, large relative deviations are observed. This behavior is primarily attributed to the fact that the absolute mass flow rates are relatively low during these transient periods. Even small absolute deviations (e.g. a few mg/s) can lead to significant relative errors under such conditions. Therefore, the more stationary period from times greater 0.22 is considered more meaningful for evaluation. Within this range, the relative deviation between simulation and measurement remains within -20 % and +5 %, with the model slightly underestimating the hydrogen mass flow. Despite this underestimation, the qualitative behavior of the mass flow rate over time is well captured by the model. When integrated over the entire refueling process, the total refueled hydrogen mass in the simulation is 5.5 % lower than the measured one.

The relative deviation of the tank pressure is also highest at the beginning of refueling, where the absolute pressure is lowest. At the point of maximum relative deviation, the simulated pressure is 3 % lower than the measured value. However, as the refueling progresses and the tank pressure increases, the relative deviation decreases. The simulated pressure remains consistently below the measured pressure throughout the process, which can be attributed to the model's presented underestimation of the mass flow rate.

Regarding tank temperature, the relative deviation between measured and simulated values remains below 0.5 % for the majority of the refueling process. A slight increase in deviation to approximately 1.5 % is observed after the refueling ends, due to post-refueling effects in the actual tank that are not captured in the simulation. Despite this, both the measured and simulated temperature curves exhibit a highly similar trend and overall behavior, indicating good agreement in the thermal dynamics of the system.

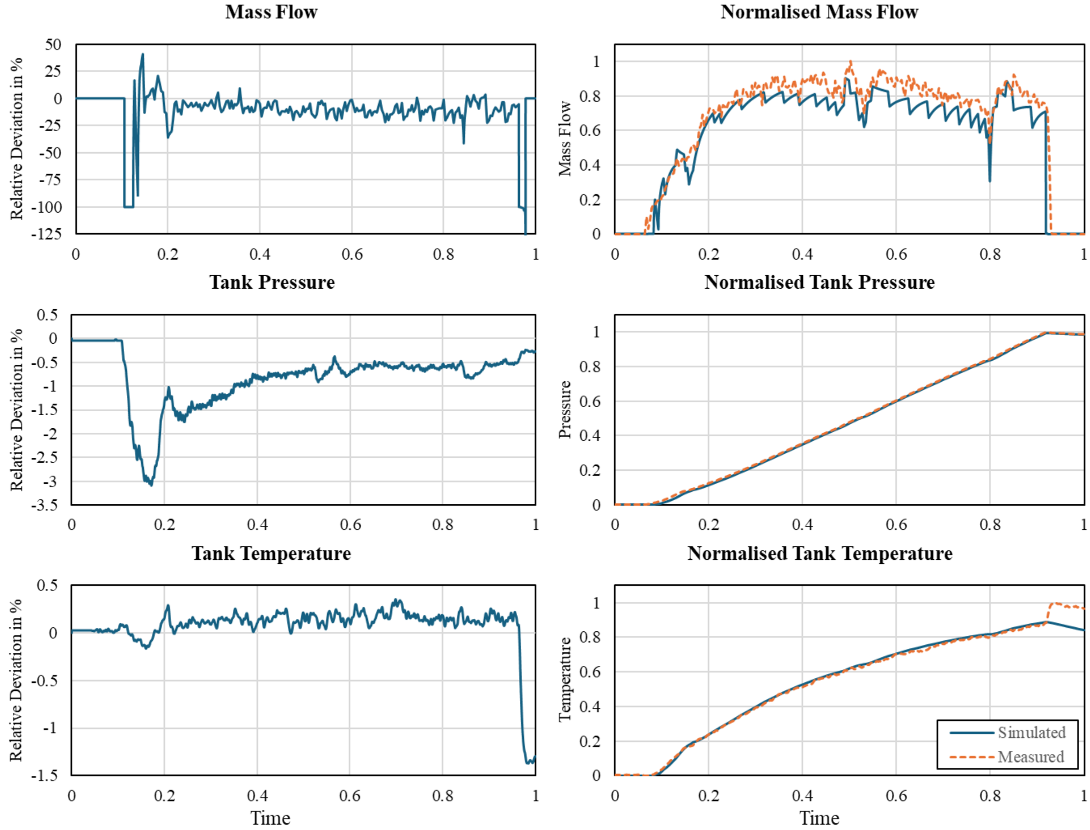

Figure 4: Relative deviation between measured and simulated values and temporal evolution of: hydrogen mass flow, pressure and temperature in the large tanks

In conclusion, the model validation process, based on a direct comparison with measurement data, demonstrates that the simulation models accurately represent the key physical processes during hydrogen refueling. The key parameters – hydrogen mass flow, tank pressure, and tank temperature – are reproduced with acceptable deviations and qualitatively consistent time-dependent behavior. The results confirm the validity of the developed models for use in further analysis and comparison of hydrogen refueling processes.

2.4 Refueling approaches

In General, different approaches are available to refill hydrogen tanks. The simplest method is to use a hydrogen trailer. The main advantage of this approach is its flexibility, as it requires no permanent infrastructure, enabling refueling directly at the train's location. However, limitations of this method are the lack of control over refueling parameters and pre-cooling. Furthermore, as the trailer's SoC decreases, both the refueling rate and the maximum achievable pressure in the vehicle decrease, leading to longer refueling times and reduced efficiency in later cycles.

For stationary hydrogen refueling stations, refueling can be controlled in two different ways, as defined in SAE J2601-5. Either by using a lookup table-based or a formula-based approach. Both can be implemented with or without communication between vehicle and station. Currently, the state-of-the-art for hydrogen-powered trains relies on lookup table-based refueling without vehicle-to-station communication. However, as previously noted, no standards are currently published defining lookup tables for the hydrogen amounts seen in hydrogen train refueling. Consequently, such tables are custom-developed for each train fleet, leading to increased development effort.

When the table-based approach is used and vehicle-to-station communication is not available, the station determines a fixed, pre-calculated pressure ramp rate based on vehicle nominal working pressure (e.g. H35), ambient temperature, vehicle hydrogen capacity category, pre-cooling temperature and initial vehicle tank pressure. This ramp rate is applied without any adjustments until the station reaches a pre-determined target pressure, ending the refueling process. If vehicle-to-station communication is available, vehicle tank pressure and temperature are exchanged during refueling. The dispenser continuously monitors the safety-critical limits based on this feedback and aborts refueling if any of these limits are exceeded, allowing the station to refuel up to an increased target pressure. Furthermore, under specific conditions (0.5 MPa < p_{init} < 5 MPa; $T_{Ambient}$ > 0 °C) a modified strategy, called top-off, is used, which reduces the ramp rate for the last part of refueling to reach a higher end-of-fill SoC. [23], [27]

In contrast to the table-based refueling method, the MC formula-based (MCF) approach defined in SAE J2601-5 employs a dynamic pressure ramp rate (PRR), recalculated every second during the refueling process. In theory, this adaptive strategy enables faster refueling compared to the table-based method, as it allows for changes in the refueling profile in response to changing conditions. The following equations form the basis of this approach [23]:

$$PRR = \frac{P_{final} - P_{ramp}}{t_{final} * \left(\frac{P_{final} - P_{initial}}{P_{final} - P_{min}}\right) - t} \; in \; MPa/s \tag{2}$$

$$P_{ramp_{j+1}} = P_{ramp} + PRR \; in \; MPa \tag{3}$$

The PRR is determined as a function of multiple variables: the final pressure ($P_{final} = 43.75$ MPa), the ramp pressure (P_{ramp}; ideal dispenser pressure), the initial vehicle tank pressure ($P_{initial}$), the minimum initial tank pressure (P_{min}), the elapsed time (t) and a continuously calculated final time (t_{final}; estimated time at which P_{final} is reached). The determination of t_{final} is central to the MCF method and involves interpolation from lookup tables, adjustment by correction factors (α, β, ε) and a lower bound (t_{final_min}) to ensure the peak mass flow rate is not exceeded. Two implementation options for interpolation of t_{final} are available [23]:

- Option A (Advanced): t_{final} is determined based on the largest individual tank volume (TVL) category and interpolated over ambient temperature and total storage system volume (V_{TS})
- Option B (Basic): t_{final} is determined based on TVL and V_{TS} category and interpolated over ambient temperature

Ultimately, the resulting t_{final} is expressed as a function of the mass-averaged temperature of the hydrogen exiting the dispenser, called MAT_C, a key thermodynamic parameter derived from real-time sensor measurements. This temperature-dependent t_{final} ensures that the refueling profile adapts to varying thermal conditions. Finally, the dispenser pressure at the next time step is then updated by adding PRR to the previous P_{Ramp} (Eq. 3). [23]

As illustrated in Figure 5, the value of t_{final} directly influences the refueling dynamics. A reduction in t_{final} accelerates the refueling process, while an increase leads to a more conservative, slower fill.

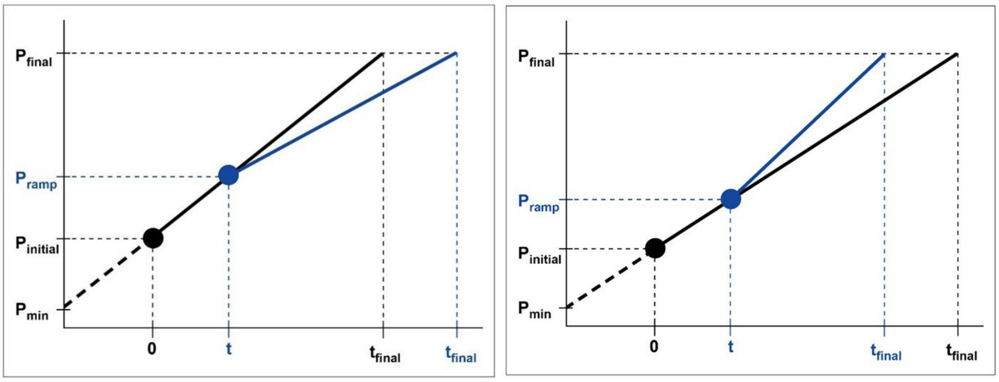

Figure 5: Effect on pressure path: left – t_{final} increase; right – t_{final} decrease [23]

For the purposes of this study, the MCF refueling logic was implemented with certain simplifications. Notably, fault detection routines were omitted to streamline the simulation. Additionally, the pre-cooling temperature was held constant throughout the refueling cycle. In the model, Option A was employed for communication refueling scenarios, while the non-communications cases used a generic t_{final} table applicable to both Option A and B.

3 Results

The following simulations were conducted in this study. Unless otherwise specified, the base conditions included an ambient temperature of 15 °C, an initial vehicle SoC of 15 %, an end of fill vehicle pressure of 350 bar – chosen to maintain a safety margin to the maximum permissible pressure – and no pre-cooling:

- Trailer refueling with 350/500 bar trailer: trailer tanks modeled as single integrated section; four consecutive refueling operations simulated
- Segmented trailer refueling with 500 bar trailer: trailer divided into three equal segments; switching between segments when pressure difference between vehicle and current trailer-segment dropped below 20 bar, five consecutive refueling operations simulated
- Ramp rate refueling without communication: 1.3 MPa/min (lowest ramp rate for H35 according to SAE J2601-5 [23])
- Ramp rate refueling (SAE J2601-5 [23], H35 Cat. D HF): 2.1 MPa/min, 40 °C ambient temperature, -20 °C pre-cooling temperature, initial vehicle pressure 50 bar, station side end of refueling condition 367 bar
- MCF refueling (SAE J2601-5 [23], H35 MCF-HF-G): simulations performed with and without communication, 40 °C ambient temperature, -20 °C pre-cooling temperature, initial vehicle pressure 50 bar

Furthermore, for the trailer refuelings a minimum mass flow of 1.25 g/s is defined, which is selected in accordance with SAE J2601-5 based on the assumption that the vehicle storage system capacity is not determined. If the mass flow falls below this threshold, it is treated as if a pressure equalization between trailer and vehicle is achieved and the simulation is stopped.

Figure 6 presents a comparative analysis of mass flow and pressure evolution in the vehicle and the trailer/refueling station during ramp rate refueling with a 1.3 MPa/min ramp, as well as the first refueling using a 350 bar and 500 bar trailer. The differences in mass flow behavior are evident. Under ramp rate refueling, the mass flow increases gradually over time, reaching a peak near the end of the process before decreasing. In contrast, during trailer refueling, the mass flow is highest at the beginning and decreases as the trailer pressure declines.

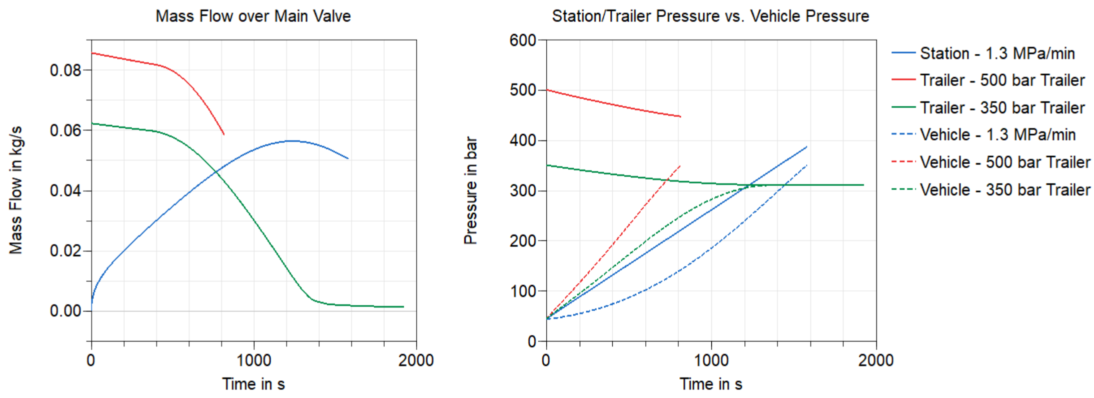

Figure 6: Mass flow and pressure evolution for ramp rate and trailer refueling

The refueling metrics for all three refuelings are provided in detail in Table 3.

Table 3: Key-Metrics for comparison of ramp rate and trailer refueling (single segment trailer)

	1.3 MPa/min	**350 bar**	**500 bar**
End of fill SoC in %	88.5	82.8	87.3
End of fill vehicle pressure in bar	350	311	350
Refueling time in min	26.4	32.1	13.6
Refueled SoC per minute in %/min	2.8	2.1	5.3

All three refueling operations remained within the safety-critical limits specified by the established refueling standards. In particular, none of the refuelings exceeded a hydrogen temperature of 75 °C. The duration of the ramp rate refueling was approximately 26.4 min, representing a reduction of about 6 min compared to the 350 bar trailer refueling, but an increase of roughly 13 min relative to the 500 bar trailer refueling. Notably, only the ramp rate and 500 bar trailer refueling achieved a complete fill of the vehicle to the target pressure of 350 bar. The 350 bar trailer refueling was terminated prematurely due to pressure equalization between the vehicle and the trailer, occurring at approx. 311 bar. As shown in Figure 6 (right), the refueling process was halted when the mass flow dropped below 1.25 g/s.

Thus, a key limitation of trailer-based refueling – relative to ramp rate refueling – is the potential inability to reach the target vehicle pressure, depending on the initial pressure in the trailer. This issue will be further examined in the following section.

Table 4 presents the results of consecutive refueling operations using a non-segmented and segmented 500 bar trailer. Using a non-segmented trailer, the first three refueling cycles were performed without any significant change in the vehicle SoC. Only minor differences are observed, which can be attributed to the lower hydrogen temperature in the vehicle resulting from the reduced refueling speed. It therefore has a higher density and thus higher SoC. The only relevant observed change was an increase in refueling duration, which can be attributed to the decreasing initial pressure in the trailer following prior refueling events. As the initial pressure in the trailer decreases, the refueling process becomes progressively slower. Therefore, the third refueling cycle was approximately 34 % longer than the first. Starting with the fourth refueling cycle, the final vehicle pressure was slightly lower compared to the first three cycles. However, the SoC remained comparable to that of the initial refueling, again caused by the lower hydrogen end of fill temperature. The primary drawback of the fourth refueling cycle is the significantly increased refueling duration, which is approximately 130 % longer than that of the first cycle. This is partially caused by the termination criterion, which was 1.25 g/s. An earlier termination could have resulted in a shorter refueling process, without significant SoC reduction. For instance, the pressure difference between the trailer and the vehicle falls below 1 bar after approximately 22.6 min. At this point, continuing the refueling would have led to a process duration roughly 65 % longer than the first cycle, indicating that earlier termination could significantly improve efficiency without compromising the achievable SoC.

Table 4: Key-Metrics of consecutive refueling processes using two types of 500 bar trailer

Number of consecutive refuelings:		1	2	3	4	5
Single segment	End of fill SoC in %	87.3	87.9	88.6	87.4	-
	End of fill vehicle pressure in bar	350	350	350	334	-
	Refueling time in min	13.6	15.5	18.4	31.6	-
	Refueled SoC per minute in %/min	5.3	4.7	4.0	2.3	-
Three equal segments	End of fill SoC in %	88.9	88.6	88.8	89.0	88.8
	End of fill vehicle pressure in bar	350	350	350	350	350
	Refueling time in min	16.9	19.7	22.4	25.4	26.7
	Refueled SoC per minute in %/min	4.4	3.7	3.3	2.9	2.8

The segmented trailer behaves similarly to the non-segmented version, yet it maintains the ability to achieve the target vehicle pressure of 350 bar even beyond the fourth refueling cycle. This demonstrates that the primary advantage of segmentation lies in the increased usable hydrogen capacity of the trailer, enabling more hydrogen to be transferred to the vehicle compared to the non-segmented configuration. The main drawback is a slightly longer refueling duration relative to the non-segmented trailer. However, this trade-off can be mitigated through optimization of the segment switching timing, offering a potential means to balance refueling speed and hydrogen utilization efficiency.

The results of the formula-based versus table-based refueling strategies are summarized in Table 5. All three refueling operations remained within the safety-critical limits specified by the SAE J2601-5 standard. In particular, none of the refuelings exceeded a hydrogen temperature of 72 °C. During the ramp rate refueling without communication, the refueling process ended after about 15 min, when the refueling station reached the target pressure of 367 bar. This same pressure threshold also ended the MCF-based refueling without communication. However, the formula-based control logic led to a steeper pressure ramp (approx. 2.55 MPa/min), causing the target pressure to be reached earlier (after 12.4 min). As a result, the MCF refueling without communication achieved a vehicle SoC of only about 56 %, which is roughly 8 % lower than the value obtained with the table-based approach under identical conditions. In terms of refueling speed (SoC per minute), both methods performed similarly, achieving 3.3 %/min.

Table 5: Key-Metrics of table and formula-based refueling approach comparison

	2.1 MPa/min	MCF non comm.	MCF comm.
End of fill SoC in %	64.8	56.4	100
Refueling time in min	15.1	12.4	19.4
Refueled SoC per minute in %/min	3.3	3.3	4.3

As expected, only the MCF refueling with communication enables a complete refueling to 100 % SoC. The process is terminated once the vehicle reaches the calculated target pressure. Furthermore, this refueling method is significantly faster than the other two cases when evaluated by SoC per minute. Due to the communication, refueling can be done less conservative utilizing an overall similar average pressure ramp rate (approx. 2.53 MPa/min) compared to the MCF non-communication method, but being able to uphold refueling for much longer and thus reaching higher SoC, showing the main strength of vehicle-to-station communication. Without communication, the refueling process must be conducted conservatively to ensure that no safety-critical parameters are exceeded. This requires stopping the process prematurely to remain within safe operating limits at all times under all conditions. In contrast, with vehicle-to-station communication, the risk of exceeding safety limits is reduced, as the process can be interrupted at any time if necessary. This allows for a smaller safety margin, improving refueling efficiency without compromising safety. However, given that the communicated parameters are safety-critical, the certification of the infrared interface defined in SAE J2799 for use in the railway sector poses a regulatory challenge.

The following key observations can be summarized:

- Larger vehicle tanks reach higher hydrogen temperatures due to worse heat transfer, resulting in a lower SoC compared to smaller tanks.
- Trailer refueling can be faster than ramp rate refueling when initial trailer pressure is sufficiently high, but performance degrades with consecutive refueling operations, reducing speed and achievable SoC. Therefore, ramp rate refuelings are more favorable for repeated refuelings.
- Segmented trailers enable more consecutive refuelings while maintaining target vehicle pressure, although they are slightly slower in early cycles compared to non-segmented trailers.
- Without communication the MCF-based refueling method achieves a lower SoC compared to the table-based approach due to earlier termination caused by a steeper ramp rate.
- The MCF approach with vehicle-to-station communication enables the safest and most efficient refueling in terms of safety compliance and achievable SoC.

4 Conclusions and Contributions

This study presents a comparison of various hydrogen refueling strategies for rail vehicles, focusing on refueling performance and safety compliance. To Benchmark different strategies, a lumped-parameter simulation model, validated against real-world data from the "Wasserstoffschiene Heidekrautbahn" project, is used. The results show that no single refueling method universally outperforms the others, rather the optimal choice depends on the specific use case. The tested refueling methods allowed for refuelings from 56 % up to 100 % SoC, with a maximum refueling speed of 5.3 %/min reaching the end of fill condition in under 14 min.

Trailer-based refueling offers flexibility and low infrastructure requirements, making it suitable for temporary deployment. However, its performance declines with consecutive refuelings due to decreasing trailer pressure, limiting refueling speed and achievable final vehicle pressure. While initial refueling events can be faster than ramp rate refuelings the inability to consistently reach the target pressure limits its suitability for long time usage. Segmented trailers mitigate this limitation by enabling more consecutive refueling cycles while maintaining the ability to reach the target pressure. Although they exhibit a slightly slower refueling speed in early cycles compared to single segment trailers. Among stationary refueling approaches, the MCF-based method with vehicle-to-station communication emerges as the most effective strategy. It enables a complete refueling to 100 % SoC thanks to real-time feedback that allows for safe, dynamic control. Using the MCF method, this is not achievable without communication. Here, a similar ramp rate compared to the refueling with communication paired with early termination results in significantly lower SoC even when compared to the table-based method without communication.

In summary, the findings underscore that future refueling infrastructure should move towards vehicle-to-station communication. Such systems will be essential to ensure safe and fast refueling of hydrogen trains. However, this requires a revision of the current standards, as the intended communication interface does not comply with the safety requirements necessary for rail vehicles.

Acknowledgements

Accompanying DLR research funded by the Ministry for Economic Affairs, Labour, Energy and Climate Action of the state of Brandenburg, Germany (MWAE) under individual measure according to the ZiFoG program, application no: 80259660, duration: 08/2022-12/2035. The vehicle data of the Siemens Mireo Plus H is collected and provided exclusively for scientific purposes as part of the research project.

References

[1] Allianz pro Schiene e.V. "Elektrifizierung erklärt: Das Schienennetz muss unter Strom stehen." Accessed: Mar. 5, 2026. [Online]. Available: https://www.allianz-pro-schiene.de/themen/infrastruktur/elektrifizierung-bahn/

[2] Eisenbahnen und Verkehrsbetriebe Elbe-Weser GmbH. "Weltpremiere: Erste Wasserstoffzüge fahren in Bremervörde." Accessed: Mar. 5, 2026. [Online]. Available: https://www.evb-elbe-weser.de/weltpremiere-erste-wasserstoffzuege-fahren-in-bremervoerde/

[3] Kreiswerke Barnim GmbH. "Wasserstoffschiene Heidekrautbahn - Das Gesamtprojekt." Accessed: Mar. 5, 2026. [Online]. Available: https://wasserstoffschiene-heidekrautbahn.de/projekt#kreiswerke-barnim

[4] Niederbarnimer Eisenbahn-AG. "Wasserstoff im Brandenburger Zugverkehr." Accessed: Mar. 19, 2026. [Online]. Available: https://www.neb.de/wasserstoffzug/

[5] Niederbarnimer Eisenbahn-AG, "Heidekrautbahn (RB27): Reaktivierung der Stammstrecke," Accessed: Mar. 19, 2026. [Online]. Available: https://www.neb.de/fileadmin/redakteure/Unternehmen/Stammstrecke/Flyer_Brosch%C3%BCren/NEB_Flyer_Heidekrautbahn_2023-06.pdf

[6] M. Böhm *et al.,* "Wasserstoffschiene Heidekrautbahn | Leitfaden 1 - Erkenntnisse aus der Betriebsvorbereitungsphase 2022-2024," 2025. [Online]. Available: https://elib.dlr.de/213239/

[7] Clean Energy Partnership e.V., "Factsheet | Refueling Protocols," Aug. 2025. Accessed: Mar. 5, 2026. [Online]. Available: https://cep.expert/wp-content/uploads/2025/09/CEP-FACTS-Refuelling_Protocols_EN.pdf

[8] R. Wurster *et al.,* "Regulatorik: Status quo und Entwicklungsbedarf," 2025. Accessed: Mar. 5, 2026. [Online]. Available: https://www.now-gmbh.de/wp-content/uploads/2025/10/NOW_Studie_Regulatorik-Wasserstoffbetankung.pdf

[9] M. Greisel and M. Gebhard, "Minimum Ambient Precooling (MAP) Hydrogen Refueling Protocol for 35MPa Heavy Duty Vehicles (20-42.5 kg)," 2022. Accessed: Mar. 5, 2026. [Online]. Available: https://cep.expert/wp-content/uploads/2025/09/CEP_REC_Fueling-Protocol-for-35-MPa-Heavy-Duty-Vehicles-20-42.5kg_Wenger-Engineering_EN.pdf

[10] V. Mattelaer, "H2 Fuelling Standards," [Online]. Available: https://interreg-baltic.eu/wp-content/uploads/2024/04/HyTruck-H2-Fuelling-Standards-Vincent-Mattelaer.pdf

[11] *SAE J2799:2024-06 - Hydrogen Surface Vehicle to Station Communications Hardware and Software,* SAE International, Warrendale, PA, United States.

[12] Siemens Mobility GmbH. "Der Weg ist bereitet für den Mireo Plus H." Accessed: Mar. 19, 2026. [Online]. Available: https://www.mobility.siemens.com/global/de/unternehmen/storys/alternative-antriebe-der-weg-ist-bereitet-fuer-den-mireo-plus-h.html

[13] M. Loncar, A. Lüschen, K. Meltzer, and M. Rahmani, "Siemens Mireo: Start in den Fahrgastbetrieb mit alternativen Antriebsarten," *eb*, vol. 123, 7-8, pp. 290–300, 2025.

[14] Siemens Mobility GmbH. "Hybrid-Triebzüge: Mireo Plus B, Mireo Plus H." Accessed: Mar. 19, 2026. [Online]. Available: https://assets.new.siemens.com/siemens/assets/api/uuid:f186839a-effd-4cef-a85b-00d84b0871fd/siemens-mobility-mireoplus-b-mireo-plus-h-de.pdf

[15] C. Mager, "Mireo Plus: Ein Hochleistungs-Brennstoffzellen-Batterie-Antrieb in einem Traktionsbaukastensystem," *45. Schienenfahrzeugtagung, Graz, Austria*, 2019.

[16] S. Wieser, L. Brünner, M. Böhm, F. Heckert, S. Rubio, and M. Soto, "Limitations in the Hydrogen Refueling Process of Railway Vehicles," in *Proceedings of the Sixth International Conference on Railway Technology: Research, Development and Maintenance*, Prague, Czech Republic, J. Pombo, Ed., 2024, pp. 1–13, doi: 10.4203/ccc.7.12.3.

[17] S. Wieser, L. Brünner, M. Böhm, M. Soto, and E. J. Rodríguez, "Development, application and optimization of hydrogen refueling processes for railway vehicles," *International Journal of Hydrogen Energy*, vol. 124, pp. 331–344, 2025, doi: 10.1016/j.ijhydene.2025.04.040.

[18] A. Charolais *et al.,* "PRHYDE Deliverable D4.1: Report on Preliminary Simulations," Jul. 2020. [Online]. Available: https://lbst.de/wp-content/uploads/2022/09/PRHYDE_Deliverable-D4-1_Report-on-Preliminary-Simulations_final_revised.pdf

[19] I. H. Bell, J. Wronski, S. Quoilin, and V. Lemort, "Pure and Pseudo-pure Fluid Thermophysical Property Evaluation and the Open-Source Thermophysical

Property Library CoolProp," *Industrial & engineering chemistry research*, early access. doi: 10.1021/ie4033999.
[20] M. Wetter, W. Zuo, T. S. Nouidui, and X. Pang, "Modelica Buildings library," *Journal of Building Performance Simulation*, vol. 7, no. 4, pp. 253–270, 2014, doi: 10.1080/19401493.2013.765506.
[21] *J2601/2_202307 - Fueling Protocol for Gaseous Hydrogen Powered Heavy Duty Vehicles,* SAE International, Warrendale, PA, United States.
[22] CMB.TECH. "500 bar mobile refueller." Accessed: Mar. 19, 2026. [Online]. Available: https://cmb.tech/h2-infra/500bar-mobile-refueller
[23] *J2601/5_202502 - High-Flow Prescriptive Fueling Protocols for Gaseous Hydrogen Powered Medium and Heavy-Duty Vehicles,* SAE International, Warrendale, PA, United States.
[24] NPROXX, "Heavy Duty Hydrogen Tank: Type 4 Pressure Vessel Specification," Accessed: Mar. 19, 2026. [Online]. Available: https://www.nproxx.com/app/uploads/2024/01/13_NPROXX_AH-500-35_FactSheet-1.pdf
[25] P. L. WOODFIELD, M. MONDE, and Y. MITSUTAKE, "Measurement of Averaged Heat Transfer Coefficients in High-Pressure Vessel during Charging with Hydrogen, Nitrogen or Argon Gas," *JTST*, vol. 2, no. 2, pp. 180–191, 2007, doi: 10.1299/jtst.2.180.
[26] P. Stephan and K. Stephan, "Wärmeübertragung," in *Dubbel Taschenbuch für den Maschinenbau 1: Grundlagen und Tabellen*, B. Bender and D. Göhlich, Eds., Berlin, Heidelberg: Springer Berlin Heidelberg, 2020, pp. 807–824.
[27] K. Reddi, A. Elgowainy, N. Rustagi, and E. Gupta, "Impact of hydrogen SAE J2601 fueling methods on fueling time of light-duty fuel cell electric vehicles," *International Journal of Hydrogen Energy*, vol. 42, no. 26, pp. 16675–16685, 2017, doi: 10.1016/j.ijhydene.2017.04.233.